Detecting heavy Higgs bosons from natural SUSY at a 100 TeV hadron collider

Howard Baer[*] and Chung Kao[†]
Homer L. Dodge Department of Physics and Astronomy, University of Oklahoma, Norman, Oklahoma 73019, USA

Vernon Barger[‡]
Department of Physics, University of Wisconsin, Madison, Wisconsin 53706, USA

Rishabh Jain[§] and Dibyashree Sengupta[∥]
Department of Physics, National Taiwan University, Taipei 10617, Taiwan

Xerxes Tata[¶]
Department of Physics, University of Hawaii, Honolulu, Hawaii 96822, USA

(Received 8 December 2021; accepted 25 April 2022; published 26 May 2022)

Supersymmetric models with radiatively driven naturalness enjoy low electroweak fine tuning whilst respecting LHC search limits on gluinos and top squarks and allowing for $m_h \simeq 125$ GeV. While the heavier Higgs bosons H and A may have TeV-scale masses, the supersymmetry (SUSY)-conserving μ parameter must lie in the few hundred GeV range. Thus, in natural SUSY models there should occur large heavy Higgs boson branching fractions to electroweakinos, with Higgs boson decays to Higgsino plus gaugino dominating when they are kinematically accessible. These SUSY decays can open up new avenues for discovery. We investigate the prospects of discovering heavy neutral Higgs bosons H and A decaying into light plus heavy chargino pairs which can yield a four isolated lepton plus missing transverse energy signature at the LHC and at a future 100 TeV pp collider. We find that the discovery of heavy Higgs decay to electroweakinos via its 4ℓ decay mode is very difficult at HL-LHC. For FCC-*hh* or SPPC, we study the $H, A \to$ SUSY reaction along with dominant physics backgrounds from the Standard Model and devise suitable selection requirements to extract a clean signal for FCC-*hh* or SPPC with $\sqrt{s} = 100$ TeV, assuming an integrated luminosity of 15 ab^{-1}. We find that while a conventional cut-and-count analysis yields a signal statistical significance greater than 5σ for $m_{A,H} \sim 1.1$ TeV $-$ 1.65 TeV, a boosted decision-tree analysis allows for heavy Higgs signal discovery at FCC-*hh* or SPPC for $m_{A,H} \sim 1$ TeV $-$ 2 TeV.

DOI: 10.1103/PhysRevD.105.095039

I. INTRODUCTION

With the discovery of the 125 GeV Standard Model-like Higgs boson at the LHC [1], all the particle states required by the Standard Model (SM) have been confirmed; yet, many mysteries of nature still remain unsolved. Supersymmetric extensions of the SM are highly motivated in that they offer a solution to the gauge hierarchy problem (GHP) [2] which arises from the quadratic sensitivity of the Higgs boson mass to high-scale physics. Supersymmetry (SUSY) models are also supported indirectly by various precision measurements within the SM; the weak scale gauge couplings nearly unify under renormalization group evolution at energy scale $m_{\rm GUT} \simeq 2 \times 10^{16}$ GeV in the minimal supersymmetric Standard Model (MSSM), but not the SM [3], the measured value of top quark mass falls within the range needed to initiate a radiative breakdown of electroweak symmetry in the MSSM [4], the measured value of the Higgs boson mass $m_h \simeq 125$ GeV falls within the narrow range of MSSM predicted values [5], and precision electroweak measurements actually favor heavy SUSY over the SM [6].

[*]baer@nhn.ou.edu
[†]Chung.Kao@ou.edu
[‡]barger@pheno.wisc.edu
[§]rishabh.jain@hep1.phys.ntu.edu.tw
[∥]dsengupta@phys.ntu.edu.tw
[¶]tata@phys.hawaii.edu

Published by the American Physical Society under the terms of the Creative Commons Attribution 4.0 International license. Further distribution of this work must maintain attribution to the author(s) and the published article's title, journal citation, and DOI. Funded by SCOAP³.

Recent LHC searches with $\sqrt{s} = 13$ TeV and integrated luminosity $L = 139\ \mathrm{fb}^{-1}$ have put lower bounds on the mass of the gluino of about 2.2 TeV [7,8] and on the mass of top squark of about 1.1 TeV [9,10]. These limits, which have been obtained using simplified model analyses assuming that the sparticle spectrum is not compressed, fall well above upper bounds derived from early naturalness considerations [11–15]. However, the naturalness estimates from the log-derivative measurements are highly dependent on what one regards as independent parameters of the theory [16].[1] We adopt the more conservative quantity $\Delta_{\rm EW}$, that allows for the possibility of correlations among model parameters, as a measure of naturalness [17]. $\Delta_{\rm EW}$ can be extracted from Eq. (1),

$$\frac{m_Z^2}{2} = \frac{m_{H_d}^2 + \Sigma_d^d - (m_{H_u}^2 + \Sigma_u^u)\tan^2\beta}{\tan^2\beta - 1} - \mu^2, \qquad (1)$$

which relates the mass of Standard Model Z boson to SUSY Lagrangian parameters at the weak scale and is obtained from the minimization conditions of the MSSM scalar potential [18]. The electroweak fine-tuning parameter $\Delta_{\rm EW}$ is defined by

$$\Delta_{\rm EW} \equiv (\max|\text{term on RHS of Eq. 1}|)/(m_Z^2/2). \qquad (2)$$

The condition for naturalness is that the maximal contribution to the Z mass should be within a factor of several of its measured value. We consider spectra that yield $\Delta_{\rm EW} > \Delta_{\rm EW}(\max) = 30$ as fine tuned [19].

This condition then requires:

(i) the SUSY-conserving μ parameter ≈ 110 GeV–350 GeV;

(ii) the up-Higgs soft mass term $m_{H_u}^2$ may be large at high scales but can be radiatively driven to (negative) natural values $\sim -m_{\rm weak}^2$ at the weak scale;

(iii) The finite radiative correction $\Sigma_u^u(\tilde{t}_{1,2})$ has an upper bound of $(350\ \mathrm{GeV})^2$ which is possible even for $m_{\tilde{t}}$ up to 3 TeV and $m_{\tilde{g}} \approx 6$ TeV [20], compatible with LHC constraints;

(iv) the heavy Higgs masses $m_{A,H,H^\pm} \sim |m_{H_d}|$, with $|m_{H_d}|/\tan\beta \sim \frac{m_Z}{\sqrt{2}}\sqrt{\Delta_{\rm EW}}$.

We thus see that naturalness requires [21]

$$m_A \lesssim \frac{m_Z \tan\beta\sqrt{\Delta_{\rm EW}(\max)}}{\sqrt{2}}, \qquad (3)$$

and further, that for $\tan\beta \sim 5$–50, the heavy Higgs boson masses may be expected to lie in the (multi) TeV range for an electroweak fine tuning of up to a part in thirty.

The conditions mentioned above are satisfied in radiatively driven natural supersymmetric (RNS) models. One of the features of RNS models is that the heavier Higgs bosons may lie in the multi-TeV range while at least some of the electroweakinos (EWinos) are below a few hundred GeV. This means that generically we expect that in natural SUSY models the supersymmetric decay modes of the heavy Higgs bosons should be kinematically accessible, and often with branching fractions comparable to SM decay modes. If SUSY decay modes of the heavy Higgs bosons are allowed, then SM search modes will be suppressed due to the presence of the SUSY decay modes, and potentially new avenues for heavy Higgs discovery may open up. This situation was investigated previously under the supposition that the lightest EWinos were predominantly gauginolike [22]. In Ref. [23], a lucrative $A, H \to \tilde{\chi}_2^0\tilde{\chi}_2^0 \to 4\ell + \not{E}_T$ search mode was identified for LHC. However, in RNS models, we expect instead that the lightest EWinos to be dominantly Higgsino-like.

Thus, we explore here a new possible heavy Higgs discovery channel for SUSY models with light H. We identify the dominant new SUSY decay mode for heavy neutral Higgs in natural SUSY models as $H, A \to \tilde{\chi}_1^\pm\tilde{\chi}_2^\mp$ that proceeds with full gauge strength[2] (provided that the decay is kinematically allowed). Allowing for chargino cascade decays, then an analogous clean $4\ell + \not{E}_T$ signature can be found. It includes leptons from the lighter chargino decay $\tilde{\chi}_1^- \to \ell^-\bar{\nu}_\ell\tilde{\chi}_1^0$ where the final state leptons are expected to be quite soft in the chargino rest frame due to the expected small mass gap $m_{\tilde{\chi}_1^-} - m_{\tilde{\chi}_1^0}$. However, due to $m_{H,A}$ lying in the TeV range, these final state leptons may be strongly boosted and thus can potentially contribute to the signal. In this paper, we examine the particular reaction $pp \to H, A \to \tilde{\chi}_1^\pm\tilde{\chi}_2^\mp \to 4\ell + \not{E}_T$ where due to the heavy Higgs resonance, we expect $M_T(4\ell, \not{E}_T)$ to be kinematically bounded by $m_{H,A}$ (see Fig. 1). While this reaction will prove difficult to extract at HL-LHC—due in part to the several leptonic branching fractions which are required—we find that discovery in this channel should be possible at the future circular hadron collider (FCC-hh) [24] or super proton-proton collider (SPPC) [25] with $\sqrt{s} \sim 100$ TeV and 15 ab^{-1} of integrated luminosity. The FCC-hh or SPPC collider has emerged as the next target hadron collider for CERN after HL-LHC in the updated European strategy report [26].

[1] The various soft SUSY breaking terms which are adopted for the log-derivative measure are introduced to parametrize one's ignorance of how soft terms arise. In more UV-complete models such as string theory, then the various soft terms are all calculable and not independent. Ignoring this could result in an overestimate of the UV sensitivity of the theory by orders of magnitude.

[2] By full gauge strength, we only mean that the Higgs scalar-Higgsino-gaugino vertex is unsuppressed. We recognize, of course, that the overall coupling of the heavy Higgs sector to the gauge boson sector is suppressed by mixing angles in the scalar Higgs sector.

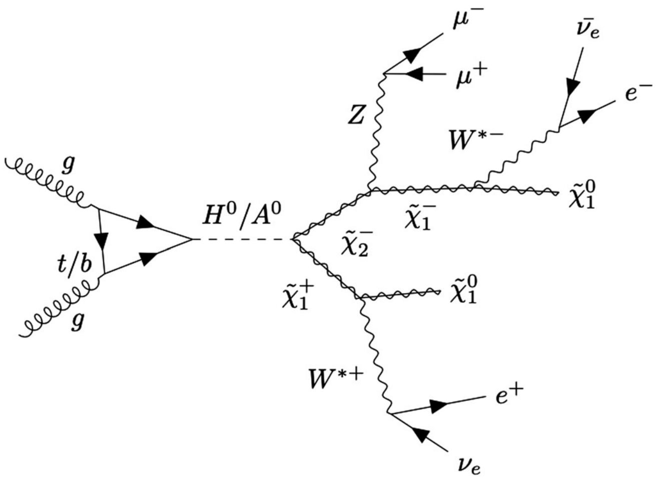

FIG. 1. Feynman diagram for $gg \to H, A(\to \tilde{\chi}_2^\pm \tilde{\chi}_1^\mp \to 4\ell + \not{E}_T) + X$ production; there is a similar diagram for H, A production via $b\bar{b}$ fusion.

To be specific, we will adopt a RNS benchmark (BM) point as listed in Table I, as generated using Isajet 7.88 [27]. This BM comes from the two extra parameter nonuniversal-Higgs model NUHM2 [28]. The NUHM2 model parameter space is given by $m_0, m_{1/2}, A_0, \tan\beta$, along with nonuniversal Higgs-mass soft terms $m_{H_u} \neq m_{H_d} \neq m_0$. Using the EW minimization conditions, it is convenient to trade the high-scale soft terms m_{H_u}, m_{H_d} for the weak-scale parameters μ and m_A. This BM point yields $m_{\tilde{g}} \simeq 2.4$ TeV, somewhat beyond the LHC lower limit of 2.2 TeV obtained from a simplified model analysis. The heavy neutral Higgs scalars have mass $m_{H,A} \sim 1.2$ TeV which is somewhat beyond the recent ATLAS limit [29] that requires $m_{H,A} \gtrsim 1$ TeV for $\tan\beta = 10$ via an $H, A \to \tau^+\tau^-$ search at $\sqrt{s} = 13$ TeV and 139 fb^{-1} of integrated luminosity (while assuming no SUSY decay modes of the heavy Higgs bosons). Also, the SUSY μ parameter is taken to be $\mu = 200$ GeV so that the BM point lies just beyond the recent analyses of the soft dilepton plus monojet Higgsino signal [30]. For the listed BM point, the lighter EWinos $\tilde{\chi}_{1,2}^0$ and $\tilde{\chi}_1^\pm$ are Higgsino-like while $\tilde{\chi}_3^0$ is binolike and $\tilde{\chi}_4^0$ and $\tilde{\chi}_2^\pm$ are winolike.

TABLE I. Input parameters (TeV) and masses (GeV) for a SUSY benchmark point from the NUHM2 model with $m_t = 173.2$ GeV using Isajet 7.88 [27].

Parameter	NUHM2
m_0	5 TeV
$m_{1/2}$	1.0 TeV
A_0	−8.3 TeV
$\tan\beta$	10
μ	200 GeV
m_A	1.2 TeV
$m_{\tilde{g}}$	2423 GeV
$m_{\tilde{u}_L}$	5293 GeV
$m_{\tilde{u}_R}$	5439 GeV
$m_{\tilde{e}_R}$	4804 GeV
$m_{\tilde{t}_1}$	1388 GeV
$m_{\tilde{t}_2}$	3722 GeV
$m_{\tilde{b}_1}$	3756 GeV
$m_{\tilde{b}_2}$	5150 GeV
$m_{\tilde{\tau}_1}$	4727 GeV
$m_{\tilde{\tau}_2}$	5097 GeV
$m_{\tilde{\nu}_\tau}$	5094 GeV
$m_{\tilde{\chi}_1^\pm}$	208.4 GeV
$m_{\tilde{\chi}_2^\pm}$	856.7 GeV
$m_{\tilde{\chi}_1^0}$	195.4 GeV
$m_{\tilde{\chi}_2^0}$	208.5 GeV
$m_{\tilde{\chi}_3^0}$	451.7 GeV
$m_{\tilde{\chi}_4^0}$	867.9 GeV
m_h	125.0 GeV
$\Omega_{\tilde{z}_1}^{std} h^2$	0.011
$BF(b \to s\gamma) \times 10^4$	3.2
$BF(B_s \to \mu^+\mu^-) \times 10^9$	3.8
$\sigma^{SI}(\tilde{\chi}_1^0, p)$ (pb)	3.1×10^{-9}
$\sigma^{SD}(\tilde{\chi}_1^0, p)$ (pb)	6.1×10^{-5}
$\langle\sigma v\rangle\|_{v\to 0}$ (cm^3/ sec)	2.0×10^{-25}
Δ_{EW}	25.5

A. Review of some previous related work and plan for this work

SUSY Higgs boson decays to EWinos were first calculated in Baer *et al.* [31]. A more comprehensive treatment was given in Gunion *et al.* [32] and Gunion and Haber [33]. Griest and Haber [34] considered the effect of invisible Higgs decays $H \to \tilde{\chi}_1^0 \tilde{\chi}_1^0$. In Kunszt and Zwirner Ref. [35], the phenomenology of SUSY-Higgs bosons in the m_A vs. $\tan\beta$ plane with just SM decay modes was considered in light of the important radiative corrections to m_h. The m_A vs. $\tan\beta$ plane was mapped including the effects of Higgs to SUSY decays in Baer *et al.* [22] considered diminution of SM Higgs decay channels due to SUSY modes along with the potential for new discovery channels arising from the SUSY-decay modes. In Ref. [23], the discovery channel $H, A \to \tilde{\chi}_2^0 \tilde{\chi}_2^0 \to 4\ell + \not{E}_T$ was examined. In Djouadi *et al.* [36], SUSY decays of heavy Higgs bosons at e^+e^- colliders were considered. Barger *et al.* [37] examined s-channel production of SM and SUSY-Higgs bosons at muon colliders. In Belanger *et al.* [38], SUSY decays of Higgs bosons at LHC were examined. Choi *et al.* [39] examined the effects of CP violating phases on Higgs to SUSY decays. In Ref. [40], a CMS study of $H, A \to \tilde{\chi}_2^0 \tilde{\chi}_2^0 \to 4\ell + \not{E}_T$ was performed. In Ref. [41], signals from $H, A \to 4\ell + \not{E}_T$ were examined including all SUSY cascade decays of heavy-Higgs bosons in scenarios where the $\tilde{\chi}_1^0$ was binolike. In Bae *et al.* [21], the impact of natural SUSY with light Higgsinos on

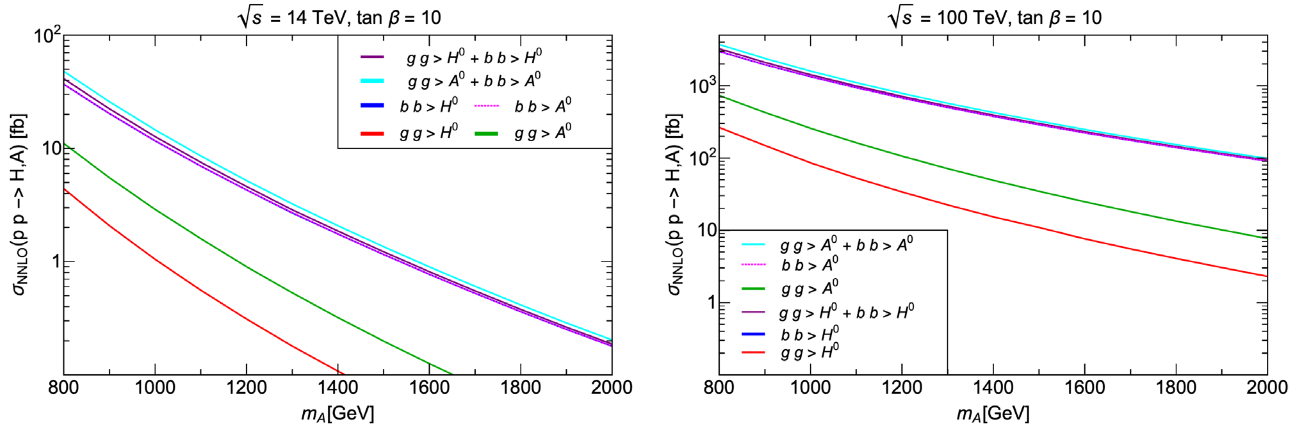

FIG. 2. $\sigma_{\mathrm{NNLO}}(pp \to H, A + X)$ for s-channel heavy neutral Higgs boson production reactions via gg and $b\bar{b}$ fusion versus m_A for (a) $\sqrt{s} = 14$ and (b) $\sqrt{s} = 100$ TeV. We take $\tan\beta = 10$. Results are from SusHi [48,49].

SUSY-Higgs phenomenology was examined and natural regions of the m_A vs. $\tan\beta$ plane were displayed along with relevant SUSY-Higgs branching fractions. The LHC-SUSY-Higgs signatures $H, A \to mono - X + \not{E}_T$ (where $X = W$, Z, h) were examined against huge SM backgrounds. In Bae *et al.* Ref. [42], the effect of natural SUSY on Higgs coupling measurements κ_i was examined. In Barman *et al.* [43], SUSY Higgs branching fractions and $mono - X + \not{E}_T$ signatures were examined at the LHC for several benchmark points along with a Higgs to SUSY trilepton signature. In Ref. [44], six MSSM-SUSY-Higgs benchmark points were proposed for LHC search studies, including one with a low, natural value of μ (which seems now to be LHC excluded). Gori, Liu, and Shakya examined SUSY-Higgs decays to EWinos and to stau pairs in Ref. [45]. In Adhikary *et al.* [46], Higgs decay to EWinos at the LHC were examined—especially the $Z + \not{E}_T$ and $h + \not{E}_T$ signatures along with the possibility of Higgs decays to long-lived charged particles (LLCPs).

B. Plan for this paper

In the present paper we examine Higgs decays to SUSY particles in natural SUSY models with light Higgsinos. In particular, in light of the large SM backgrounds for $mono - X + \not{E}_T$ searches, we examine the viability of resurrecting the $H, A \to 4\ell + \not{E}_T$ signature. In the natural SUSY case, this signature could arise from $H, A \to \tilde{\chi}_1^\pm \tilde{\chi}_2^\mp$ followed by $\tilde{\chi}_2^\pm \to Z\tilde{\chi}_1^\pm$. The $Z \to \ell^+\ell^-$ decay should be easily visible but the leptons from $\tilde{\chi}_1^- \to \ell\nu_\ell\tilde{\chi}_1^0$ are typically very soft in the $\tilde{\chi}_1^\pm$ rest frame. Owing to the TeV scale values of $m_{H,A}$, these otherwise soft leptons may be boosted to detectable levels. While such a complicated decay channel appears intractable at HL-LHC, the FCC-*hh* or SPPC operating at $\sqrt{s} \sim 100$ TeV and 15 ab^{-1} should allow for discovery for $m_{H,A} \sim 1$ TeV $- 2$ TeV with advanced machine learning (ML) techniques; here we have used boosted decision trees as an illustration.[3]

The remainder of this paper is organized as follows. In Sec. II, we present s-channel production rates for heavy Higgs bosons at LHC14 and at FCC-*hh* or SPPC. In Sec. III, we discuss the heavy Higgs branching fractions that are expected in natural SUSY models and we motivate our particular four lepton SUSY-Higgs discovery channel. In Sec. IV, we discuss leading SM backgrounds to the $H, A \to 4\ell + \not{E}_T$ signal channel. In Sec. V, we perform a cut-based analysis while in Sec. VI we show one can do much better by invoking a boosted-decision-tree (BDT) analysis. In Sec. VII, we summarize our main conclusions.

II. HEAVY HIGGS PRODUCTION AT LHC AND FCC-HH OR SPPC

Here, we will focus on the s-channel heavy neutral Higgs boson production reactions $pp \to H, A$ which occurs via the gluon-gluon and $b\bar{b}$ fusion subprocesses. Other reactions such as $pp \to qqH$ (VV fusion reactions) WH, ZH, and $t\bar{t}H$ all occur at lower rates [47] and also lead to different final-state topologies. Hence, we will not include these in our analysis.

In Fig. 2 we show the heavy neutral Higgs production cross sections at next-to-next-to-leading order (NNLO) in QCD. We adopt the SusHi program [48–58] to generate these results, which include QCD corrections and effects from top and bottom squark loops. Higher-order QCD corrections typically boost these cross sections above their leading order estimates. Frame (a) shows results for

[3]Since one of our goals is to illustrate how ML techniques may help to eke out a signal that lies below the discovery limit using standard cut-and-count analyses if the Higgs boson is very massive, we have confined our study to the signal in this single channel, and for simplicity carried out our calculations using parton level simulations.

$\sqrt{s} = 14$ TeV while frame (b) shows results for $\sqrt{s} = 100$ TeV. We see that even for $\tan\beta = 10$, heavy Higgs boson production via $b\bar{b}$ fusion dominates that from gluon fusion. From frame (a), we see that for $m_A \sim 800$ GeV, the total production cross sections occur for both H and A production at the $\sim$40 fb level. As m_A increases, the rates fall and are already below the 0.2 fb level for $m_A \gtrsim 2$ TeV. We can anticipate that once we fold in various leptonic branching fractions and include detector acceptances, we will not expect very high rates for multi-lepton signals from heavy neutral SUSY Higgs bosons at LHC14. In frame (b), we show the results for $\sqrt{s} = 100$ TeV. Here, the cross sections are increased by factors of 70–500 as m_A varies from 800 GeV–2000 GeV.

III. HEAVY HIGGS AND SPARTICLE BRANCHING FRACTIONS

In this section we present some updated heavy neutral and charged Higgs branching fractions which we extract from the Isajet 7.88 code [27]. We adopt the benchmark point from Table I except now we allow the heavy Higgs mass m_A to vary. In frame (a), we show branching fractions for the heavy neutral scalar H. At low m_H, the SM modes $H \to b\bar{b}$, $\tau\bar{\tau}$, and $t\bar{t}$ are dominant, with their exact values depending on $\tan\beta$ (large $\tan\beta$ enhances the $b\bar{b}$ and $\tau\bar{\tau}$ modes). For $m_H \sim 400$ GeV $-$ 650 GeV, the SM modes are still dominant even though the light electroweakino modes are open. We can understand this by examining the Higgs sector Lagrangian in the notation of Ref. [18] (Sec. VIII. 4)

$$\mathcal{L} \ni -\sqrt{2}\sum_{i,A} \mathcal{S}_i^\dagger g t_A \bar{\lambda}_A \frac{1-\gamma_5}{2}\psi_i + \text{H.c.} \tag{4}$$

where $\mathcal{S}_i$ labels various matter and Higgs scalars (labeled by i), ψ_i is the fermionic superpartner of $\mathcal{S}_i$, and λ_A is the gaugino with gauge index A. Also, g is the gauge coupling for the gauge group and t_A are the corresponding gauge-group generator matrices. Letting $\mathcal{S}_i$ be the Higgs scalar fields, then we see that the Higgs-EWino coupling is maximal when there is little mixing in that the Higgs fields couple directly to gaugino plus Higgsino. Back in Fig. 3(a), for m_H small, then the only open decay modes are H to Higgsino plus Higgsino, and so the coupling must be dynamically suppressed because the gaugino component of the lightest EWinos is very small. Thus the SM modes are still dominant. As m_H increases, then the decay to gaugino plus Higgsino turns on and the above coupling is unsuppressed (as has also been noted in footnote 2). For our

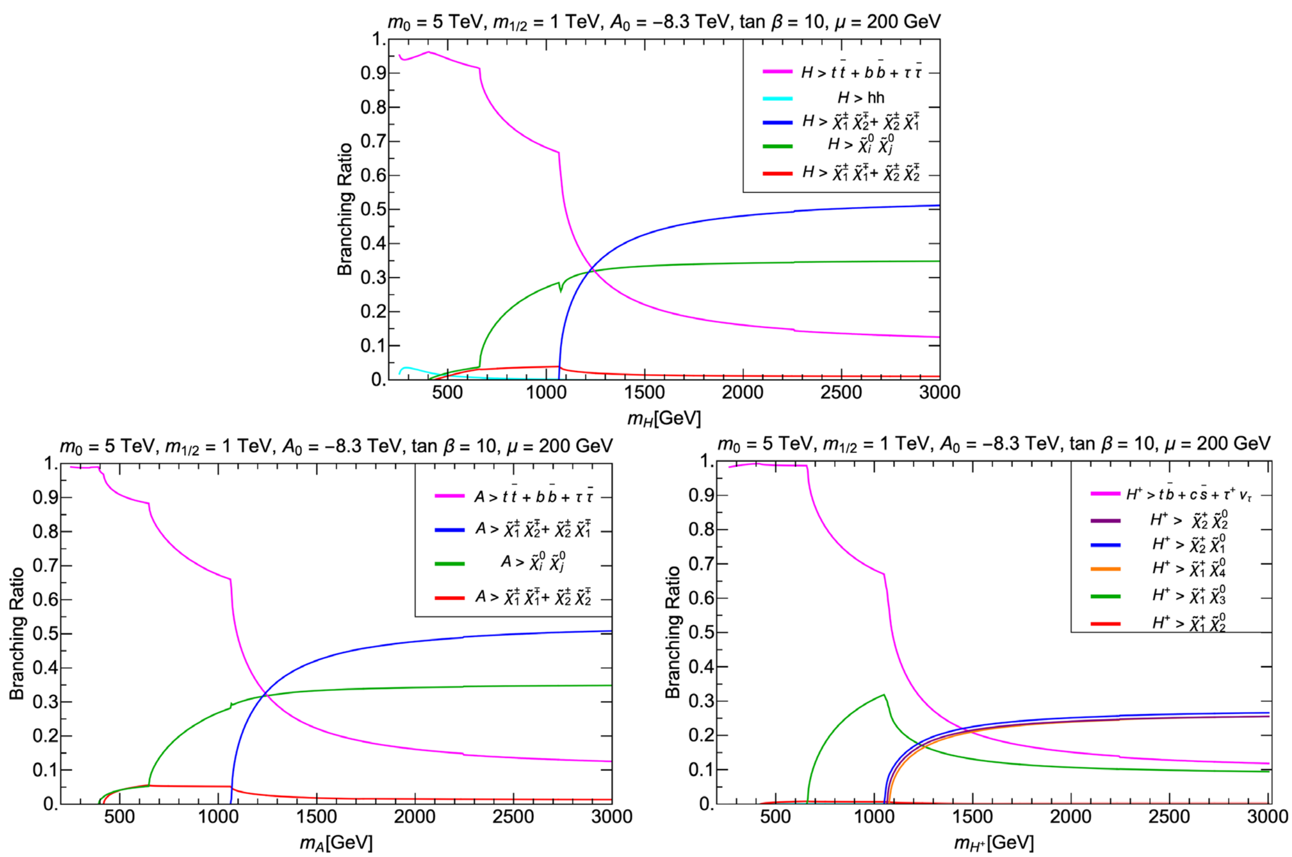

FIG. 3. Branching fractions versus heavy Higgs mass for $a)$ H, $b)$ A and $c)$ H^+ into SM and SUSY particles in the NUHM2 model with $\mu = 200$ GeV and $m_0 = 5$ TeV, $m_{1/2} = 1$ TeV, $A_0 = -8.3$ TeV and $\tan\beta = 10$.

TABLE II. Dominant branching fractions for heavy Higgs H, A for the benchmark point with $m_A = 1200$ GeV.

Decay mode	Branching fraction
$H \to b\bar{b}$	22.5%
$H \to \tilde{\chi}_1^\pm \tilde{\chi}_2^\mp$	31.2%
$H \to \tilde{\chi}_2^0 \tilde{\chi}_4^0$	12.2%
$A \to b\bar{b}$	22.9%
$A \to \tilde{\chi}_1^\pm \tilde{\chi}_2^\mp$	30.0%
$A \to \tilde{\chi}_1^0 \tilde{\chi}_4^0$	12.2%

choice of SUSY parameters, this happens around $m_H \sim 650$ GeV for H decay to Higgsino plus bino and around $m_H \sim 1050$ GeV for H decay to wino plus Higgsino. Since the latter coupling involves the larger $SU(2)_L$ gauge coupling, the decay $H \to$ wino plus Higgsino ultimately dominates the branching fraction once it is kinematically allowed. Thus, for $m_H \gtrsim 1250$ GeV, $H \to \tilde{\chi}_1^\pm \tilde{\chi}_2^\mp$ dominates the branching fraction (blue curve), while decays of H to the lighter neutral Higgsino-like neutralino plus the heavier neutral wino or binolike neutralino (green curve) have a branching fraction about half as large. In this range of m_H, the SM H decay modes are severely depressed from their two-Higgs doublet (non-SUSY) expectation. This will make heavy Higgs detection via $t\bar{t}$, $b\bar{b}$ and $\tau\bar{\tau}$ much more difficult. On the other hand, it opens up new discovery channels by searching for the dominant $H \to$ EWino modes.

In Fig. 3(b), we show the same branching fractions except now for the pseudoscalar A. The branching fractions look qualitatively similar to those in frame (a) since the same reasoning applies. Thus, the A will decay mainly to SM modes for smaller values of m_A even though decays to Higgsino-like pairs are available. It is only when decays to gaugino plus Higgsino open up that the branching fractions to SUSY modes begin to dominate.

For completeness, we also show in Fig. 3(c) the branching fractions for charged Higgs decays H^+. As in the previous cases, H^+ decay to SM modes $t\bar{b}$ and $\tau^+\nu_\tau$ dominate at low values of m_{H^+} even though decay to $\tilde{\chi}_1^+ \tilde{\chi}_{1,2}^0$ modes are kinematically allowed. As m_{H^+} increases, then decays to $\tilde{\chi}_1^+ \tilde{\chi}_3^0$ (Higgsino-bino) followed by $\tilde{\chi}_2^+ \tilde{\chi}_{1,2}^0$ and $\tilde{\chi}_4^0 \tilde{\chi}_1^+$ (Higgsino-wino) turn on and rapidly dominate the decays.

Some dominant heavy neutral Higgs decay branching fractions are shown in Table II for the benchmark point shown in Table I. We see again that for the benchmark point the H and A decays to SM modes are suppressed compared to decay rates into gaugino plus Higgsino.

In Fig. 4 we combine the H and A production rates from Fig. 2 with the Higgs boson and sparticle branching fractions to the $4\ell + \not{E}_T$ final state depicted in Fig. 1. We see from Fig. 4(a) that, for $\tan\beta = 10$, even without cuts we expect *at most* ~7 signal events at HL-LHC, assuming an integrated luminosity of 3000 fb^{-1}. Moreover, we expect that this will be reduced considerably once detector efficiency and analysis cuts are folded in. However, as we can see from frame (b), the raw signal cross section is larger at the higher-energy FCC-*hh* or SPPC by a factor 150–500 (compared to LHC14), so that with the projected 15 ab^{-1} of integrated luminosity, we may hope to be able to extract an observable signal even after cuts. We will, therefore, mostly focus our attention on a 100 TeV pp collider in the remainder of this paper.

The reader may be concerned that our dismissal of the possibility of a signal in the $4\ell + \not{E}_T$ channel at LHC14 was based on the event rate for $\tan\beta = 10$ when it is well known that the couplings of the A and H both increase with $\tan\beta$, resulting in an increased rate for H/A production from bottom quark fusion. It should, however, be remembered that the range of m_A excluded by the current upper limit on the cross section times branching ratio for the decay $\phi \to \tau\bar{\tau}$ ($\phi = A, H$) also increases with $\tan\beta$ for this

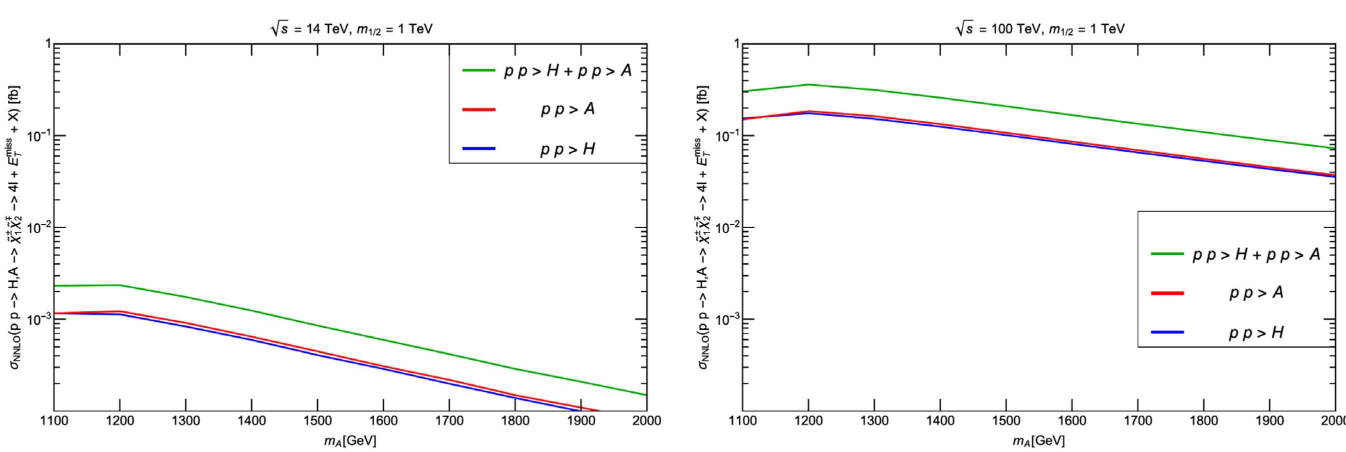

FIG. 4. NNLO Cross sections from SusHi $\sigma(A)$, $\sigma(H)$, and $\sigma(A) + \sigma(H)$ times the cascade decay branching fractions into the $4\ell + \not{E}_T$ final state in fb vs. m_A for (a) 14 TeV and (b) 100 TeV without any cuts.

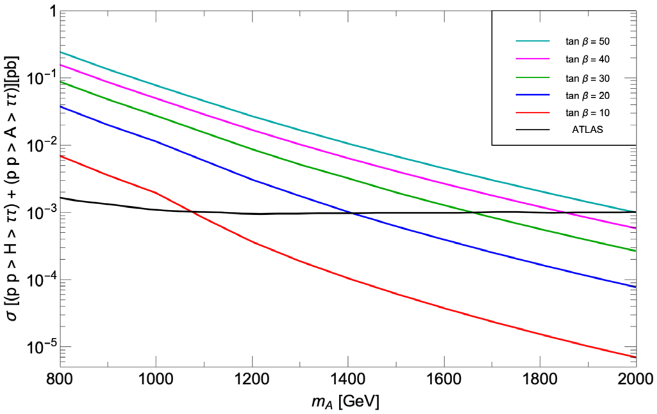

FIG. 5. The summed cross section times branching ratio for $A/H \to \tau\bar{\tau}$ versus m_A at LHC14 for several values of $\tan\beta$. Other parameters are fixed at their values for the model line introduced in the text. The horizontal black line shows the current upper limit on the cross section obtained by ATLAS.

same reason. This is illustrated in Fig. 5 where we show the expectations for the resonant production of tau pairs from the decay of $H/A \to \tau\bar{\tau}$ versus m_A for several values of $\tan\beta$. Other parameters are taken to be the same as for the model-line introduced earlier. The horizontal black line is the current ATLAS upper bound on this rate [29]. We see that while $m_A > 1.1$ TeV for $\tan\beta = 10$, for $\tan\beta = 50$, $m_A > 2$ TeV. Scaling the cross section in the left frame of Fig. 4 by the ratio of the corresponding values of $\tan^2\beta$ still leaves us with just a handful of events before cuts at the HL-LHC for currently allowed values of m_A.

IV. SM BACKGROUNDS AND ANALYSIS CUTS

Our signal $pp \to H, A \to \chi_1^{\pm}\chi_2^{\mp} \to 4\ell + \not{E}_T$ contains 4 leptons and missing energy in the final states, where one pair of leptons comes from the decay of a Z-boson. Since, as just mentioned, the signal rate is too small at the HL-LHC, we will from now on mostly focus our attention on a 100 TeV pp collider.

Our simplified study has been carried out at parton level. The dominant SM background to the $4\ell + \not{E}_T$ events comes from $W^{\pm}W^{\mp}V$, $t\bar{t}V$, Zh, and ZZV ($V = W^{\pm}, Z, \gamma$). Notice that the partonic final states from the signal, as well as from all the backgrounds other than $t\bar{t}V$ production, are free of any hadronic activity. We use tree-level matrix elements from the HELAS library in Madgraph to evaluate the backgrounds, and then scale our cross section to NLO with K-Factors calculated using MCFM [59].[4] For the $t\bar{t}V$ background we veto events which contain any b-jets (i.e., b-quarks) with $p_T > 20$ GeV and $|\eta(b)| < 2.5$. This serves as a powerful cut in reducing this background. However, with PDF enhancements, we find that this background becomes the second most dominant background at $\sqrt{s} = 100$ TeV. $W^{\pm}W^{\mp}V$ proves to be the most dominant background at all energies.

To select events, we identify the isolated leptons if they satisfy

(i) p_T (ℓ_1, ℓ_2, ℓ_3, ℓ_4) > 20 GeV, 10 GeV, 10 GeV, 10 GeV;
(ii) $|\eta|$ (ℓ_1, ℓ_2, ℓ_3, ℓ_4) < 2.5.

We model experimental errors in the measurement of lepton energies by Gaussian smearing electron and muon energies using [60],

$$\frac{\Delta E}{E} = \frac{0.25}{\sqrt{\mathrm{E(GeV)}}} \oplus 0.01, \tag{5}$$

where $\oplus$ denotes addition in quadrature.

Since the signal of interest has a final state of $4\ell + \not{E}_T$, we started with a set of minimal cuts, labeled as Cuts A, which include:

(i) Veto events with b-jets p_T (jet) > 20 GeV and $|\eta|$ (jet) < 2.5 as already mentioned;
(ii) $\Delta_R(j, \ell) > 0.4$, where j denotes a b-quark with $p_T < 20$ GeV or with $|\eta_b| > 0.4$, to mimic lepton isolation;
(iii) Invariant mass for two opposite sign same flavor leptons $M_{\ell^+\ell^-} > 10$ GeV, to reduce the background from $\gamma^* \to \ell\bar{\ell}$;
(iv) $\not{E}_T > 125$ GeV.

After applying cut A, the mass distributions and $\not{E}_T$ distribution obtained (upon summing $b\bar{b}$ and gg initiated processes) are shown in Figs. 6 and 7, respectively.

Since neutralinos and neutrinos escape detection (and so serve as sources of missing energy) it is not possible to reconstruct the invariant mass of H or A as a bump in the invariant mass of the final state. We can, however, sharpen the signal by additional cuts. Motivated by [61], we apply $\not{E}_T \geq 275$ GeV cut, since we have two neutralinos of mass ~100 GeV in the final state. As can be seen from Figs. 6 and 7, the following mass cuts and $\not{E}_T$ cuts can reduce the SM background very efficiently. Further cuts applied are

(i) We define ℓ_1 and ℓ_2 as the two leptons whose invariant mass is closest to m_Z and require $|M(\ell_1, \ell_2) - m_Z| < 10$ GeV since the signal includes one Z boson[5];
(ii) $10 < M(\ell_3, \ell_4) < 75$ GeV, where ℓ_3 and ℓ_4 denotes the remaining leptons.
(iii) $0.14 m_A < M(4\ell) < 0.34 m_A$
(iv) $\not{E}_T > 275$ GeV.

Of course, since m_A is not known *a priori*, the cut on $M(4\ell)$ needs further explanation. Unless m_A has already been measured from studies of A or H decays via SM channels, operationally, m_A here refers to the upper end

[4]The K-factors that we use are, $K_{WWV} = 1.36$, $K_{t\bar{t}V} = 1.30$, $K_{Zh} = 1.40$, and $K_{ZZV} = 1.40$.

[5]Although we do not explicitly require it, for the most part, ℓ_1 and ℓ_2 have opposite sign and same flavor.

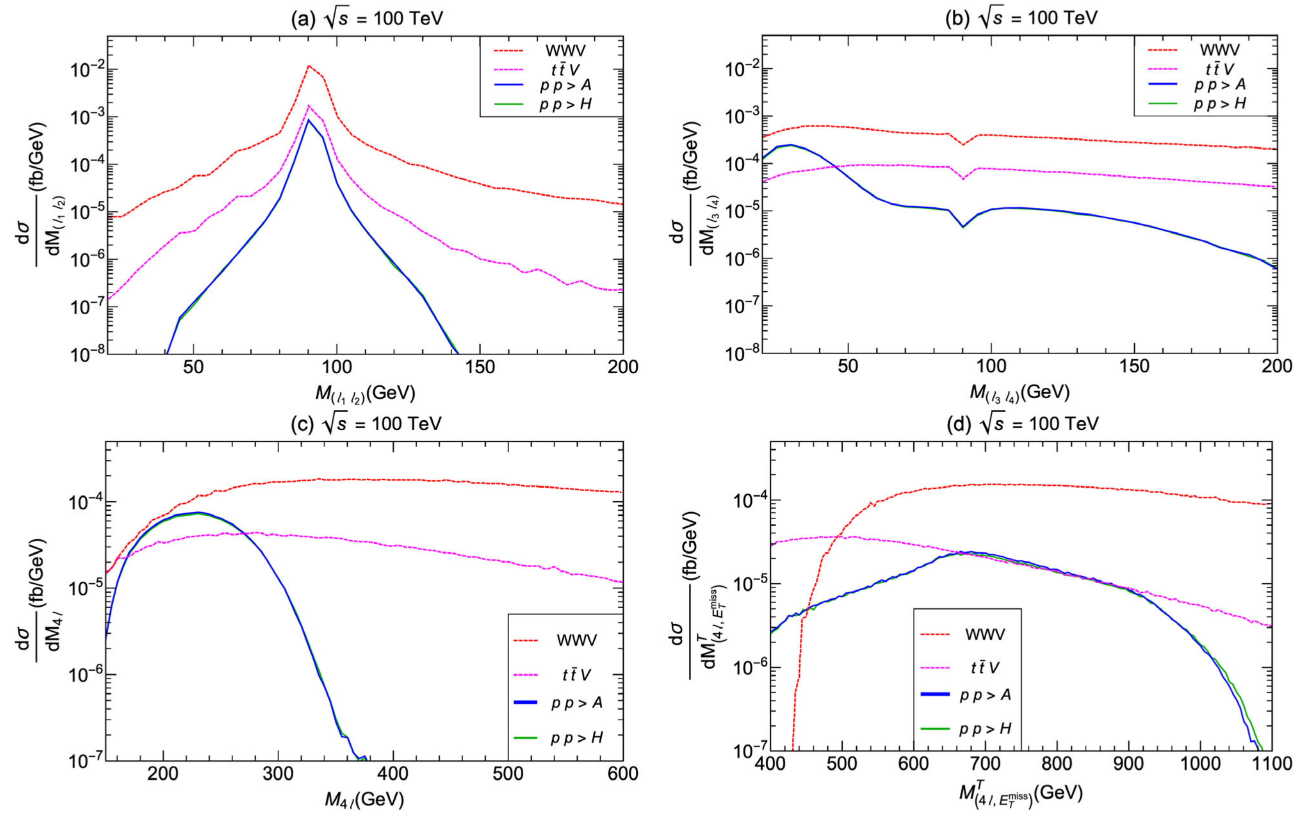

FIG. 6. Plots of the (a) invariant mass distribution $M(\ell_1, \ell_2)$ of the two leptons that form an invariant mass closest to m_Z, (b) invariant mass distribution of the remaining two leptons, $M(\ell_3, \ell_4)$, (c) invariant mass of the 4ℓ system, and (d) cluster transverse-mass distribution of the $4\ell + \not{E}_T$ system, for the Higgs signal $(pp \to H, A \to 4\ell + \not{E}_T + X)$, after the cut set A defined in the text. The corresponding contributions from the dominant physics backgrounds are also shown.

point of the signal $M_T(4\ell, \not{E}_T)$ distribution shown in frame (d) of Fig. 6, assuming that it can be experimentally extracted.[6] We note that the optimal choice of the $M(4\ell)$ cut would only be weakly sensitive to the lightest neutralino mass for $m_{A,H} \gg m_{\tilde{\chi}_1^0}$. The cut set A, augmented by the cuts listed above, is labeled as cut set B.

In Fig. 8 we show the signal cross section versus m_A after cuts B at (a) the HL-LHC, and (b) a 100 TeV pp collider. We indeed see from frame (a) that for all values of m_A the signal lies well below the one-event level. Although perhaps only of academic interest, it is worth noting that a comparison of this figure with Fig. 4(a) shows that the signal efficiency is ~5%–10% despite the requirement all four leptons are required to have a p_T of at least 10 GeV. This is a reflection of the boost the electroweakinos, and concomitantly the leptons, gain when they originate in the decays of the heavy Higgs bosons. From Fig. 8(b), we project that at the FCC or at the SPPC with an integrated luminosity of 15 ab^{-1}, several tens of signal events may be expected after cuts B over most of the range of m_A in the figure.

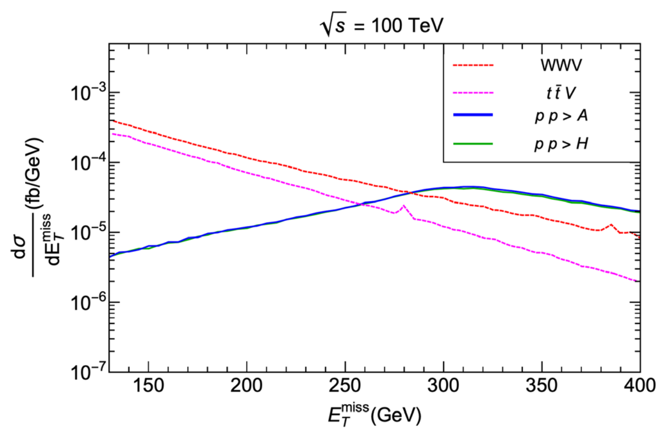

FIG. 7. The missing transverse energy $\not{E}_T$ distribution for the Higgs signal $(pp \to H, A \to 4\ell + \not{E}_T + X)$ after the cuts set A. The corresponding contributions from the dominant physics backgrounds are also shown.

[6]We appreciate that the extraction of this end point may be very difficult. Since this is a first exploration of the $4\ell + \not{E}_T$ signal from the decay of heavy Higgs bosons in natural SUSY models, we do not attempt to explore the details of the end point determination, but simply assume that it can be extracted from the data.

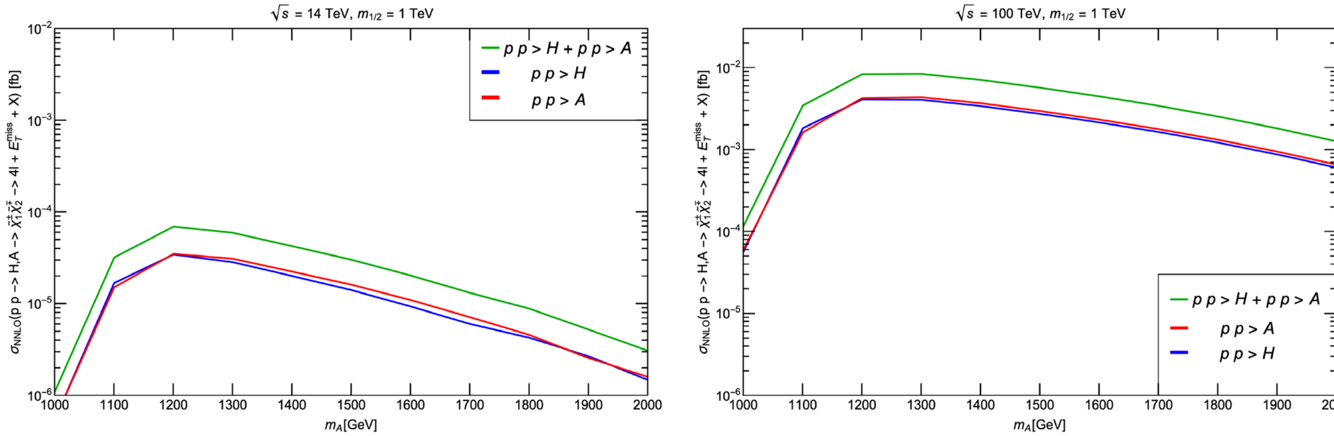

FIG. 8. NNLO Cross sections, $\sigma(A)$, $\sigma(H)$, and $\sigma(A)+\sigma(H)$ times the cascade decay branching fractions into the $4\ell + \not{E}_T$ final state in fb vs. m_A for (a) 14 TeV and (b) 100 TeV, after the cut set B defined in the text.

V. DISCOVERY POTENTIAL WITH CUT-AND-COUNT ANALYSIS

In this section we study the discovery potential of the $4\ell + \not{E}_T$ signal for heavy Higgs bosons at a 100 TeV pp collider using a traditional cut-and-count analysis. To this end, we show in Table III our results for the signal after the cut set B for three benchmark points (BPs) with varying m_A (with other parameters fixed to their values in Table I), along with the main sources of SM backgrounds. The subdominant background listed in the fourth-last row is the combined background resulting from SM Zh and from ZZV production.

In Fig. 9 we present our estimates of statistical significance [62],

$$N_{ss} \equiv \sqrt{(2\times(N_S+N_B)\ln(1+N_S/N_B) - 2\times N_S)},$$

for 1100 GeV $\leq m_A \leq$ 2000 GeV. Our selection cuts work well in removing a large part of the background. We see that with a center-of-mass energy of 100 TeV and integrated luminosity of $\mathcal{L} = 15\ \mathrm{ab}^{-1}$, we have enough events to claim a 5σ discovery for $m_A \sim 1.1$ TeV – 1.65 TeV. We also obtain a 95% C.L. exclusion limit for the $H, A \to 4\ell + \not{E}_T$ signal for values of m_A extending out as far as 2 TeV.

We now turn to an examination of whether we can use machine learning techniques to suppress the background further and concomitantly increase the reach. In the next section we study the use of boosted decision trees to further enhance the signal.

TABLE III. The signal and SM background cross section in fb at a 100 TeV pp collider for three benchmark points after the cut set B defined in the text. All the cross sections are in fb. Here, N_S is the total number signal events, combining both scalar and pseudo scalar and N_B is the total number of background events and N_{ss} is the statistical significance of the signal, all for an integrated luminosity of 15 ab^{-1}. We have all flavors of leptons (e and μ).

	BP1 $m_A =$ 1200 GeV	BP2 $m_A =$ 1400 GeV	BP3 $m_A =$ 1600 GeV
$pp \to H$	4.12×10^{-3}	3.45×10^{-3}	2.17×10^{-3}
$pp \to A$	4.38×10^{-3}	3.73×10^{-3}	2.35×10^{-3}
$W^+W^-\ell^+\ell^-$	7.13×10^{-3}	7.23×10^{-3}	6.18×10^{-3}
$t\bar{t}\ell^+\ell^-$	1.83×10^{-3}	1.58×10^{-3}	1.17×10^{-3}
$Z\ell^+\ell^-\ell^+\ell^-$	1.38×10^{-3}	1.41×10^{-3}	1.24×10^{-3}
N_S	127	108	68
N_B	155	153	129
N_{ss}	9.1	7.9	5.5

VI. IMPROVEMENT WITH BOOSTED DECISION TREES

We have just seen that the cut-based signal from heavy Higgs boson decays via the $4\ell + \not{E}_T$ channel yields a statistically significant discovery level over a limited range of m_A values even at a 100 TeV pp collider. Of course, it is possible that this signal may be combined with a signal

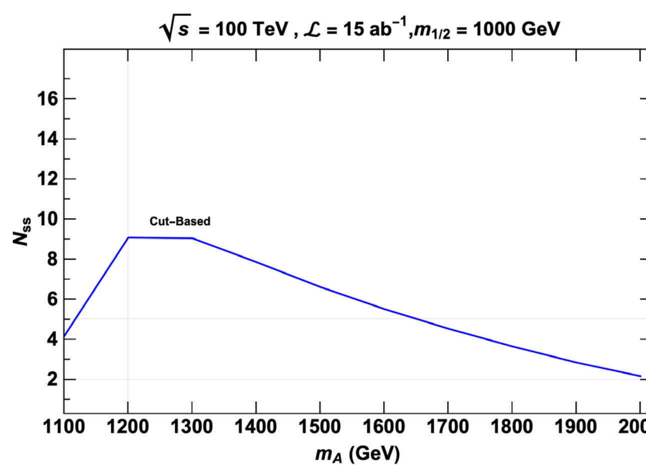

FIG. 9. The signal significance N_{ss} vs. m_A using a traditional cut-based analysis for $pp \to H + A \to 4\ell + \not{E}_T$ events at a 100 TeV pp collider.

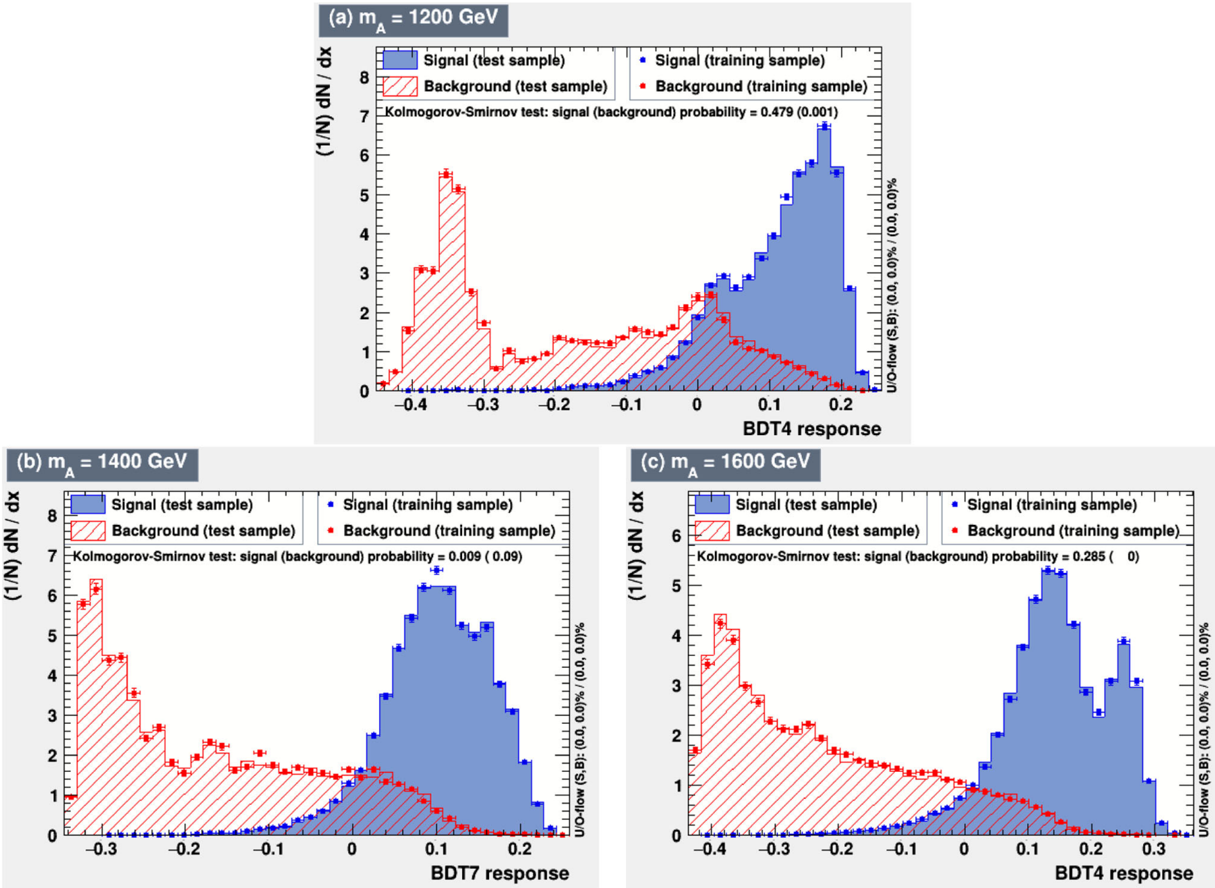

FIG. 10. The BDT response for $m_A =$ (a) 1200, (b) 1400, and (c) 1600 GeV. The BDT response of test points (solid) and training points (with error bar) is superposed in the figure.

from other channels to claim discovery over a wider range. The point of this study, however, is to examine how much improvement may be possible without combining other channels if we go beyond the traditional cut-based analysis which as we saw yields a discovery significance of $N_{ss} > 5$ for $m_A \sim 1.1$ TeV $-$ 1.65 TeV for $\sqrt{s} = 100$ TeV and 15 ab^{-1} of integrated luminosity.

It has been found that ML techniques can greatly improve the signal-to-background discrimination and they are widely used by experimental analyses. In this section we use boosted decision trees (BDT) for which algorithms are included in the ToolKit for MultiVariate Analysis [63], a multivariate analysis package included with ROOT. For this study, we have used the following variables for training and testing,

(i) The invariant mass $M(4\ell)$.
(ii) The invariant masses $M(\ell_1, \ell_2)$ and $M(\ell_3, \ell_4)$
(iii) $\not{E}_T$, missing transverse energy.

We have generated signal files for each value of m_A along with the backgrounds at 100 TeV after applying the cut set B, except that we have now relaxed the cut on $\not{E}_T$ to be $\not{E}_T > 200$ GeV before passing the samples for training and testing. We train 400,000 signal events and 400,000 background events for each channel. We used the same number of events for testing. Figure 10 shows the BDT response for three BPs with different m_A values.

In Table IV, we present our estimate of N_{ss} from the BDT analysis for the same BP points as in Table III. We see that there is, indeed, a significant improvement over the previous cut-based analysis.

Figure 11 shows the individual contributions from each of H and A for the BDT analysis along with the significance from the combined H and A signal. This may be compared

TABLE IV. A comparison between the cut-based and BDT analyses for the three benchmark points introduced in the text.

Number of events	pp $\to \phi^0$	Total background	N_{ss}
	BP1, $m_A = 1200$ GeV		
All mass cuts	127	155	9.1
BDT cut	132	58	13.7
	BP2, $m_A = 1400$ GeV		
All mass cuts	107	153	7.9
BDT cut	133	46	14.9
	BP3, $m_A = 1600$ GeV		
All mass cuts	68	129	5.5
BDT cut	72	25	11.0

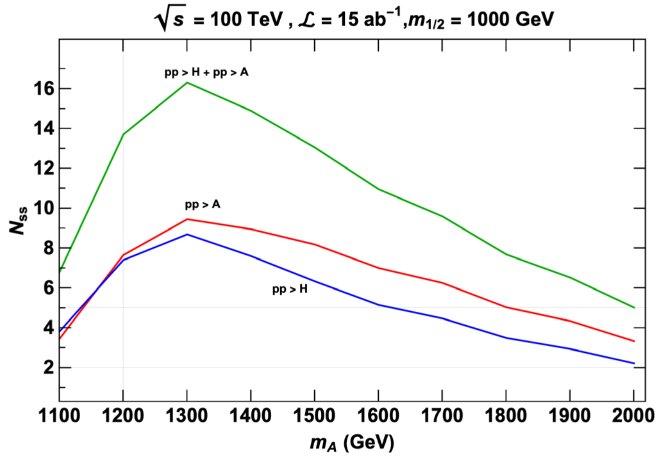

FIG. 11. Statistical significance plots for the $H, A \to 4\ell + \not{E}_T$ signal at a 100 TeV hadron collider after the BDT analysis.

to the significance shown in Fig. 9 for the traditional cut-and-count analysis. We see that, by using the BDT analysis, we would be able to discover H and A at the 5σ level via $H, A \to 4\ell + \not{E}_T$ channel for $m_A \sim 1$ TeV − 2 TeV; a considerable improvement in range of m_A over the usual cut-based method.

VII. CONCLUSIONS

In this paper, we have examined heavy neutral Higgs boson discovery as motivated by natural SUSY models with light Higgsinos. In such models, the heavy Higgs H, A decays to electroweakinos are almost always open since the lightest Higgsinos are expected to have masses below ~350 GeV range whilst the H and A bosons can have TeV-scale masses. Since decays to pairs of Higgsino-like states are dynamically suppressed, our channel of primary interest is $H, A \to \tilde{\chi}_1^{\pm}\tilde{\chi}_2^{\mp}$ decay, followed by $\tilde{\chi}_2^{\pm} \to Z\tilde{\chi}_1^{\pm}$ followed by $Z \to \ell^+\ell^-$ and then each $\tilde{\chi}_1^{\pm} \to \ell^{\pm}\nu_\ell\tilde{\chi}_1^0$. Combining all flavors of decays to e and μ leads to a distinctive $H, A \to 4\ell + \not{E}_T$ signature for heavy Higgs boson decay to SUSY particles. The leptons from $\tilde{\chi}_1^{\pm}$ decay are soft in the $\tilde{\chi}_1^{\pm}$ rest frame but are boosted to higher energies due to the large $m_{H,A}$ masses. Thus, we evaluated this signal channel against dominant SM backgrounds for both HL-LHC and for FCC-*hh* or SPPC with $\sqrt{s} = 100$ TeV, applying judicious cuts on various combinations of invariant masses of the leptons, and also requiring $\not{E}_T > 275$ GeV. Our selection requirements retain much of the signal while removing the physics background efficiently.

In our analysis we have focused on production of the heavy Higgs bosons with a mass ($m_H \simeq m_A$) between 1 TeV and 2 TeV. While a signal (in the $4\ell + \not{E}_T$ channel) is not likely to be observable at HL-LHC, prospects are much better at FCC-*hh* or SPPC. The best case for discovery is near $m_A \simeq 1.2$ TeV − 1.3 TeV that has a balance between kinematics of leptons in the final state and production cross sections. We note the following:

(i) A 100 TeV hadron collider offers promise to discover a heavy neutral Higgs boson via one of its dominant SUSY decay modes in natural SUSY models with a mass ~1 TeV − 2 TeV. With a conventional cut-based analysis, we are able to obtain a $N_{ss} > 5$ statistical significance over a range $m_A \sim 1.1$ TeV − 1.65 TeV. We find though that a BDT analysis of the same signal can potentially improve the significance greatly giving N_{ss} as high as 16 for $m_A \simeq 1.3$ TeV, and $N_{ss} > 5$ over a range $m_A \sim 1$ TeV − 2 TeV even via our proposed very difficult discovery channel.

(ii) For somewhat smaller values of heavy Higgs boson masses characterized by $m_A \lesssim 1$ TeV TeV, the signal cross section is suppressed both by smaller branching ratio into the SUSY mode, and also by a smaller boost of the daughter EWinos which, in turn, reduces the efficiency with which the softer leptons pass the cuts. Nonetheless, the heavy neutral SUSY-Higgs bosons should be detectable in this range via SM decay modes such as $H, A \to \tau\bar{\tau}$.

(iii) For increasing m_A values beyond ~1.3 TeV, the Higgs production cross section becomes much smaller since the gg and $b\bar{b}$ fusion production cross sections are increasingly suppressed.

(iv) We stress that we have focused only on the signal from a difficult SUSY decay mode of the heavy Higgs boson with an eye to assessing how ML techniques could serve to enhance difficult to see signals. Hence we have not examined the possibility of combining SUSY modes or whether the discovery of a heavy Higgs boson might be possible from a study of its SM decays.

For $m_A \simeq m_H$ significantly beyond 1 TeV and $\tan\beta \sim$ 10–50, it may become increasingly challenging to search for heavy Higgs bosons via their decays into SM particles due to the diminished branching fractions to $b\bar{b}$ and $\tau\bar{\tau}$, once the dominant SUSY decay channels become allowed. The chargino and neutralino discovery channel for heavy Higgs bosons at high energy hadron colliders offers an important opportunity to discover the heavy neutral Higgs bosons via their decay into EWinos. An upgrade to a 100 TeV hadron collider seems essential for heavy Higgs H and A discovery via the natural SUSY $4\ell + \not{E}_T$ channel.

ACKNOWLEDGMENTS

We thank an anonymous referee for useful suggestions. This work was supported in part by the US Department of Energy, Office of High Energy Physics Grants No. DE-SC-0009956 and No. DE-SC-0017647. The work of D. S. was supported in part by the Ministry of Science and Technology (MOST) of Taiwan under Grant No. 110-2811-M-002-574, and the work of R. J. is supported by MOST 110-2639-M-002-002-ASP.

[1] G. Aad *et al.* (ATLAS Collaboration), Phys. Lett. B **716**, 1 (2012); S. Chatrchyan *et al.* (CMS Collaboration), Phys. Lett. B **716**, 30 (2012).
[2] E. Witten, Nucl. Phys. **B188**, 513 (1981); R. K. Kaul, Phys. Lett. **109B**, 19 (1982).
[3] S. Dimopoulos, S. Raby, and F. Wilczek, Phys. Rev. D **24**, 1681 (1981); U. Amaldi, W. de Boer, and H. Furstenau, Phys. Lett. B **260**, 447 (1991); J. R. Ellis, S. Kelley, and D. V. Nanopoulos, Phys. Lett. B **260**, 131 (1991); P. Langacker and M. x. Luo, Phys. Rev. D **44**, 817 (1991).
[4] L. E. Ibanez and G. G. Ross, Phys. Lett. B **110B**, 215 (1982); K. Inoue, A. Kakuto, H. Komatsu, and S. Takeshita, Prog. Theor. Phys. **68**, 927 (1982); **71**, 413 (1984); L. Ibanez, Phys. Lett. **118B**, 73 (1982); H. P. Nilles, M. Srednicki, and D. Wyler, Phys. Lett. **120B**, 346 (1983); J. Ellis, J. Hagelin, D. Nanopoulos, and M. Tamvakis, Phys. Lett. **125B**, 275 (1983); L. Alvarez-Gaume, J. Polchinski, and M. B. Wise, Nucl. Phys. **B221**, 495 (1983); B. A. Ovrut and S. Raby, Phys. Lett. **130B**, 277 (1983); for a review, see L. E. Ibanez, and G. G. Ross, C. R. Phys. **8**, 1013 (2007).
[5] H. E. Haber and R. Hempfling, Phys. Rev. Lett. **66**, 1815 (1991); J. R. Ellis, G. Ridolfi, and F. Zwirner, Phys. Lett. B **257**, 83 (1991); Y. Okada, M. Yamaguchi, and T. Yanagida, Prog. Theor. Phys. **85**, 1 (1991); For a review, see e.g. M. S. Carena and H. E. Haber, Prog. Part. Nucl. Phys. **50**, 63 (2003).
[6] S. Heinemeyer, W. Hollik, and G. Weiglein, Phys. Rep. **425**, 265 (2006).
[7] The ATLAS Collaboration (ATLAS Collaboration), Report No. ATLAS-CONF-2017-022, 2017.
[8] A. M. Sirunyan *et al.* (CMS Collaboration), Phys. Rev. D **97**, 012007 (2018); A. M. Sirunyan *et al.* (CMS Collaboration), Eur. Phys. J. C **77**, 710 (2017).
[9] The ATLAS Collaboration (ATLAS Collaboration), Report No. ATLAS-CONF-2017-037, 2017.
[10] A. M. Sirunyan *et al.* (CMS Collaboration), J. High Energy Phys. 10 (2017) 019.
[11] R. Barbieri and G. F. Giudice, Nucl. Phys. **B306**, 63 (1988).
[12] S. Dimopoulos and G. F. Giudice, Phys. Lett. B **357**, 573 (1995).
[13] G. W. Anderson and D. J. Castano, Phys. Rev. D **52**, 1693 (1995).
[14] R. Kitano and Y. Nomura, Phys. Rev. D **73**, 095004 (2006); M. Papucci, J. T. Ruderman, and A. Weiler, J. High Energy Phys. 09 (2012) 035.
[15] N. Craig, arXiv:1309.0528.
[16] H. Baer, V. Barger, and D. Mickelson, Phys. Rev. D **88**, 095013 (2013); A. Mustafayev and X. Tata, Indian J. Phys. **88**, 991 (2014); H. Baer, V. Barger, D. Mickelson, and M. Padeffke-Kirkland, Phys. Rev. D **89**, 115019 (2014).
[17] H. Baer, V. Barger, P. Huang, A. Mustafayev, and X. Tata, Phys. Rev. Lett. **109**, 161802 (2012); H. Baer, V. Barger, P. Huang, D. Mickelson, A. Mustafayev, and X. Tata, Phys. Rev. D **87**, 115028 (2013).
[18] H. Baer and X. Tata, *Weak Scale Supersymmetry: From Superfields to Scattering Events* (Cambridge University Press, Cambridge, England, 2006).
[19] H. Baer, V. Barger, and M. Savoy, Phys. Rev. D **93**, 035016 (2016).
[20] H. Baer, V. Barger, J. S. Gainer, P. Huang, M. Savoy, H. Serce, and X. Tata, Phys. Lett. B **774**, 451 (2017).
[21] K. J. Bae, H. Baer, V. Barger, D. Mickelson, and M. Savoy, Phys. Rev. D **90**, 075010 (2014).
[22] H. Baer, M. Bisset, D. Dicus, C. Kao, and X. Tata, Phys. Rev. D **47**, 1062 (1993).
[23] H. Baer, M. Bisset, C. Kao, and X. Tata, Phys. Rev. D **50**, 316 (1994).
[24] F. Bordry, M. Benedikt, O. Brüning, J. Jowett, L. Rossi, D. Schulte, S. Stapnes, and F. Zimmermann, arXiv:1810.13022.
[25] M. Ahmad, D. Alves, H. An, Q. An, A. Arhrib, N. Arkani-Hamed, I. Ahmed, Y. Bai, R. B. Ferroli, Y. Ban *et al.*, Report No. IHEP-CEPC-DR-2015-01, 2015.
[26] European Strategy Group, Report No. CERN-ESU-013, 2020.
[27] F. E. Paige, S. D. Protopopescu, H. Baer, and X. Tata, arXiv:hep-ph/0312045.
[28] D. Matalliotakis and H. P. Nilles, Nucl. Phys. **B435**, 115 (1995); M. Olechowski and S. Pokorski, Phys. Lett. B **344**, 201 (1995); P. Nath and R. L. Arnowitt, Phys. Rev. D **56**, 2820 (1997); J. Ellis, K. Olive, and Y. Santoso, Phys. Lett. B **539**, 107 (2002); J. Ellis, T. Falk, K. Olive, and Y. Santoso, Nucl. Phys. **B652**, 259 (2003); H. Baer, A. Mustafayev, S. Profumo, A. Belyaev, and X. Tata, J. High Energy Phys. 07 (2005) 065.
[29] G. Aad *et al.* (ATLAS Collaboration), Phys. Rev. Lett. **125**, 051801 (2020).
[30] G. Aad *et al.* (ATLAS Collaboration), Phys. Rev. D **101**, 052005 (2020); A. Tumasyan *et al.* (CMS Collaboration), J. High Energy Phys. 04 (2022) 091.
[31] H. Baer, D. Dicus, M. Drees, and X. Tata, Phys. Rev. D **36**, 1363 (1987).
[32] J. F. Gunion, H. E. Haber, M. Drees, D. Karatas, X. Tata, R. Godbole, and N. Tracas, Int. J. Mod. Phys. A **02**, 1035 (1987).
[33] J. F. Gunion and H. E. Haber, Nucl. Phys. **B307**, 445 (1988); **B402**, 569(E) (1993).
[34] K. Griest and H. E. Haber, Phys. Rev. D **37**, 719 (1988).
[35] Z. Kunszt and F. Zwirner, Nucl. Phys. **B385**, 3 (1992).
[36] A. Djouadi, P. Janot, J. Kalinowski, and P. M. Zerwas, Phys. Lett. B **376**, 220 (1996).
[37] V. D. Barger, M. S. Berger, J. F. Gunion, and T. Han, Phys. Rep. **286**, 1 (1997).
[38] G. Belanger, F. Boudjema, F. Donato, R. Godbole, and S. Rosier-Lees, Nucl. Phys. **B581**, 3 (2000).
[39] S. Y. Choi, M. Drees, J. S. Lee, and J. Song, Eur. Phys. J. C **25**, 307 (2002).
[40] C. Charlot, R. Salerno, and Y. Sirois, J. Phys. G **34**, N1 (2007).
[41] M. Bisset, J. Li, N. Kersting, R. Lu, F. Moortgat, and S. Moretti, J. High Energy Phys. 08 (2009) 037.
[42] K. J. Bae, H. Baer, N. Nagata, and H. Serce, Phys. Rev. D **92**, 035006 (2015).
[43] R. K. Barman, B. Bhattacherjee, A. Chakraborty, and A. Choudhury, Phys. Rev. D **94**, 075013 (2016).
[44] E. Bagnaschi, H. Bahl, E. Fuchs, T. Hahn, S. Heinemeyer, S. Liebler, S. Patel, P. Slavich, T. Stefaniak, C. E. M. Wagner *et al.*, Eur. Phys. J. C **79**, 617 (2019).
[45] S. Gori, Z. Liu, and B. Shakya, J. High Energy Phys. 04 (2019) 049.

[46] A. Adhikary, B. Bhattacherjee, R. M. Godbole, N. Khan, and S. Kulkarni, J. High Energy Phys. 04 (2021) 284.

[47] S. Dittmaier *et al.* (LHC Higgs Cross Section Working Group), Report Nos. CERN-2011-002, CERN-2011-002, CERN, Geneva, 2011.

[48] R. V. Harlander, S. Liebler, and H. Mantler, Comput. Phys. Commun. **184**, 1605 (2013).

[49] R. V. Harlander, S. Liebler, and H. Mantler, Comput. Phys. Commun. **212**, 239 (2017).

[50] R. V. Harlander and W. B. Kilgore, Phys. Rev. Lett. **88**, 201801 (2002).

[51] R. V. Harlander and W. B. Kilgore, Phys. Rev. D **68**, 013001 (2003).

[52] U. Aglietti, R. Bonciani, G. Degrassi, and A. Vicini, Phys. Lett. B **595**, 432 (2004).

[53] R. Bonciani, G. Degrassi, and A. Vicini, Comput. Phys. Commun. **182**, 1253 (2011).

[54] G. Degrassi and P. Slavich, J. High Energy Phys. 11 (2010) 044.

[55] G. Degrassi, S. Di Vita, and P. Slavich, J. High Energy Phys. 08 (2011) 128.

[56] G. Degrassi, S. Di Vita, and P. Slavich, Eur. Phys. J. C **72**, 2032 (2012).

[57] R. Harlander and P. Kant, J. High Energy Phys. 12 (2005) 015.

[58] K. G. Chetyrkin, J. H. Kuhn, and M. Steinhauser, Comput. Phys. Commun. **133**, 43 (2000).

[59] R. Boughezal, J. M. Campbell, R. K. Ellis, C. Focke, W. Giele, X. Liu, F. Petriello, and C. Williams, Eur. Phys. J. C **77**, 7 (2017).

[60] The ATLAS Collaboration (ATLAS Collaboration), Report No. ATLAS-PHYS-PUB-2013-004, 2013.

[61] M. Aaboud *et al.* (ATLAS Collaboration), J. High Energy Phys. 10 (2018) 180.

[62] G. Cowan, K. Cranmer, E. Gross, and O. Vitells, Eur. Phys. J. C **71**, 1554 (2011).

[63] A. Hocker, P. Speckmayer, J. Stelzer, J. Therhaag, E. von Toerne, H. Voss, M. Backes, T. Carli, O. Cohen, A. Christov *et al.*, arXiv:physics/0703039.